Analysis of the sound radiated by a heavy fluid loaded structure excited by an impulsive force

R. Scherrer, Laurent Maxit, Jean-Louis Guyader, C. Audoly, M. Bertinier

Analysis of the sound radiated by a heavy fluid loaded structure excited by an impulsive force

Roch Scherrer [1,2], Laurent Maxit [1], Jean-Louis Guyader [1], Christian Audoly [2], Michel Bertinier [3]

[1] LVA, INSA de Lyon

25 bis Avenue. Jean Capelle, 69621 Villeurbanne Cedex, France

[2] DCNS Research, Le Mourillon

Rond-point de l'Artillerie de Marine BP 403, 83000 Toulon, France

[3] DGA TN

Avenue de la tour royale BP 40915, 83000 Toulon, France

ABSTRACT

The aim of this work consists in evaluating and analyzing vibrations and radiated pressure from a fluid loaded structure excited by a transient mechanical source. The time signature can be estimated from a discrete inverse Fourier transform of the Frequency Response Functions (FRF) of the considered system. In order to validate the numerical process, a simple structure composed of an infinite flat plate excited by an impulse point force is considered. Results are compared with an analytic result for the in-vacuo plate. When the plate is immerged on one side, the vibrations and radiated pressure from the plate are evaluated with the developed numerical process. Then, one studies the effect of the fluid loading and the dispersive nature of the flexural waves on the vibrations, and radiated pressure time signature in the far field of the plate. A comparison between Khirchoff-Love and Mindlin Timoshenko plate is also made.

Keywords: Transient Noise, Vibration

1. INTRODUCTION

The acoustic radiation of a water-loaded structure excited by an impulse force is of interest for the acoustic stealth of submarines [1-2]. In the literature, a lot of works proposed to investigate the radiation of water-loaded structure excited by stationary sources, but few attentions have been paid to the case of transient sources. Mackertich and Hayek [3] studied the acoustic radiation from an impulsively excited plate. Using the residue method, they obtained an analytical expression of the radiated pressure and they analyzed the time response in the near field of the plate. They noted that the signal contains waves travelling in both plate and fluid since the shape of the pressure is influenced by the dispersivity of the plate and the signal arrives sooner than expected for an acoustic wave travelling only in the water. Choi et al. [4] studied the acoustic radiation from a finite-length shell with substructures subjected to an impulsive excitation. They noted that the junction between the substructures and the shell creates a noise source that radiates in the far field. Leblond et al. proposed a fully elastic model based on Laplace transform for

submerged circular cylindrical shells subject to a weak shock wave, and noted that this model gives more similar results with experiments than the Khirchoff-Love model [5].

In the present paper, we propose to consider a numerical process to investigate the time response of a water loaded structure excited by an impulse force. This process is based on a resolution of the vibro-acoustic problem in the frequency-wavenumber space. The time response is obtained by achieving numerically the inverse time and space Fourier transform. This process could be applied in the future to a fluid loaded periodically stiffened panel [6-8] or to an immersed shell coupled with its internal frames [9]. In the present paper, it is applied to the basic case of an infinite fluid loaded plate. It allows us to validate the numerical process and to study the influence of different phenomena on the time response: interaction of the structure with the heavy fluid, dispersive nature of the flexural waves, structural damping (models, values), and rotational inertia/shear stress effect.

The paper is organized as follows:
- The mathematical formulation of the problem and its resolution in the wavenumber space is proposed in Sec. 2. The numerical process allowing us to deduce the time response is also given in this section;
- For validation purpose, the results obtained with the numerical process are compared in Sec. 3 with analytical results for an in-vacuo plate;
- In Sec. 4, one studies the time response of the fluid loaded plate, as well as for the plate vibration than for its radiated pressure in the far field. The influence of the different parameters described previously is discussed.

2. ESTIMATION OF THE TIME RESPONSE OF THE FLUID LOADED PLATE

2.1 Model and formulation

Let us considered an infinite plane isotropic plate which separates the space along the z=0 plane, as shown in Figure 1 in the spherical coordinate system (r, θ, ϕ). The plate is made of steel: ρ_s, D and h are respectively the density, the flexural rigidity and the thickness of the plate (for the simulation, the chosen thickness is $h = 20\ mm$). The fluid (i.e. water) is in the z>0 half space, only. ρ_0, c_0 are respectively the density and the sound speed of the fluid. The plate is excited by a normal point force at r=0. This force is an impulse at $t=0$. Its time signal is $F(r, t) = F_0 \delta(r, t)$ and its Fourier transform is $f(\omega) = \frac{f_0}{2\pi}$.
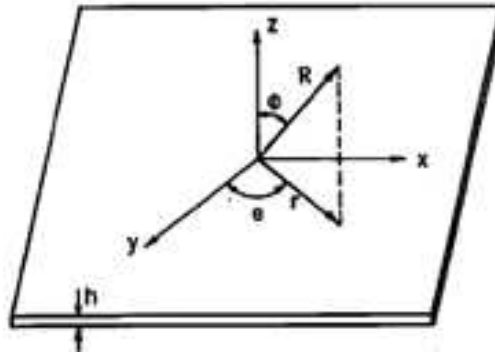

Figure 1 - Infinite plate and coordinates

The plate can be modeled by using the Mindlin-Timoshenko theory [10] which takes the rotation inertia and shear stress effects into account. In the frequency domain, the plate equation of motion is:

$$\left[\left(\nabla^2 + \frac{\rho_s h \omega^2}{D} S\right)\left(D\nabla^2 + \rho_s h \omega^2 I\right) - \rho_s h \omega^2 + 2\sqrt{\rho_s hD}\xi \frac{\partial^2}{\partial r^2}\frac{\partial}{\partial t}\right] w(r)$$
$$= \left(1 - S\nabla^2 - \frac{\rho_s h \omega^2}{D} IS\right)\frac{F_0 \delta(r)}{2\pi r} - \left(1 - S\nabla^2 - \frac{\rho_s h \omega^2}{D} IS\right) p(r)$$

(1)

Where:
- w is the transversal displacement of the plate at the angular frequency ω;

- F_0 and p, are, respectively, the external point force and the pressure exerted by the fluid on the plate;
- ξ is the viscoelastic damping factor of the plate
- The shear stress parameter S and the rotation inertia I are defined, respectively, by:

$$S = \frac{12D}{\pi^2 Gh} \tag{2}$$

$$I = \frac{h^2}{12} \tag{3}$$

The Khirchoff-Love theory can easily be found if S and I are neglected.

In this equation, one has introduced a viscoelastic damping model (i.e. damping forces proportional to the time derivative of the plate displacement) since the hysteretic damping yields to a non-causal system.

The pressure in the fluid respects the Helmholtz equation whereas the Euler equation relates the plate displacement to the pressure at the interface plate-fluid.

2.2 Resolution in the frequency-wavenumber space

The problem describes in Sec. 2.1 is resolved in the frequency-wavenumber space. The axisymmetry of the problem allows us using the Hankel transform:

$$\widetilde{w}(\gamma) = \int_0^{+\infty} w(r)J_0(\gamma r)dr \tag{4}$$

where J_o is the Bessel function of the first kind and order 0.

After some algebra, one obtains in the frequency-wavenumber space (ω, γ), the spectral displacement of the plate:

$$\widetilde{w}(\gamma) = \frac{iF}{2\pi D} \frac{g(\gamma)}{(\gamma^2 - \delta_1{}^2)(\gamma^2 - \delta_2{}^2) - 2i\sqrt{\rho_s hD}\xi\gamma^2 k_f^2 + \frac{\rho_0 \omega^2}{Dk_z}g(\gamma)} \tag{5}$$

and the spectral pressure in the fluid:

$$\widetilde{p}(\gamma, z) = \frac{\rho_0 \omega^2}{k_z}\widetilde{w}(\gamma)e^{izk_z} \tag{6}$$

with:

$$g(\gamma) = 1 + S\gamma^2 - \frac{\rho_s h\omega^2}{D}IS \tag{7}$$

$$\delta_1{}^2 = \frac{\rho_s h\omega^2}{2D}\left[I + S + \sqrt{(I-S)^2 + 4\frac{D}{\rho_s h\omega^2}}\right] \tag{8}$$

$$\delta_2{}^2 = \frac{\rho_s h\omega^2}{2D}\left[I + S - \sqrt{(I-S)^2 + 4\frac{D}{\rho_s h\omega^2}}\right] \tag{9}$$

$$k_z = i\sqrt{\gamma^2 - k_0{}^2}, \quad if \quad |\gamma| > |k_0| \tag{10}$$

$$k_z = \sqrt{k_0{}^2 - \gamma^2}, \quad if \quad |\gamma| < |k_0| \tag{11}$$

The displacement and the pressure in the physical space can be obtained using the inverse Hankel transform:

$$w(r) = \int_0^{+\infty} \widetilde{w}(\gamma)J_0(\gamma r)d\gamma \tag{12}$$

This integration cannot be calculated analytically, because one needs to find the roots of a 5th degree polynomial. This operation will be achieved numerically as developed in the next section.

2.3 Numerical process to estimate the time response

As we have used the time Fourier transform and the space Hankel transform to obtain the spectral displacement/pressure, the time response can be obtained by achieving the inverse operation of these two transforms. The numerical process is then decomposed in two steps:

- The first step consists for a given frequency to evaluate numerically the integral of (6). We use the MATLAB command *quadgk*, which implies a computation by Gauss-Kronrod quadrature [11];

- The second step corresponds to the inverse Fourier transform which is achieved by using a Fast Fourier Transform algorithm. It is necessary to truncate the frequency axis to $[-f_{max}, f_{max}]$, where f_{max} is the frequency sampling, and to discretize it with the frequency resolution δf.

For the radiated pressure in the far field, the first step is not necessary because the stationary phase theorem [12] gives us an analytical expression of the pressure in the physical space. This permits to save huge computing times.

3. VALIDATION OF THE NUMERICAL PROCESS

Let us consider the in-vacuo Love-Kirchhoff plate in order to validate the numerical process described in Sec. 2. For this case, *S=I=0* and the last term of the denominator of Eq. (3) vanishes. We can apply the numerical process like for a fluid loaded plate. On another hand, an analytical expression of the time signal of the velocity has been obtained by Guyomar *et al.* [13]:

$$\frac{\partial w}{\partial t}(r,t) = \frac{1}{2t\rho_s h}\sqrt{\frac{2\pi\rho_s h}{D(1-\xi^2)}}e^{-\frac{r^2\xi}{4t}\sqrt{\rho_s h/D}}\sin\left(\frac{r^2}{4t}\sqrt{\frac{\rho_s h}{D}(1-\xi^2)}\right) \tag{13}$$

One can observe that the two first terms of this expression describe damping effect, whereas the third term describes the dispersive nature of the flexural waves of the plate. One has v(r,0) = 0 but if t ≠0 the velocity is not zero whatever the value of the distance r is. This is due to the fact that this expression is obtained considering a perfect impulse force with a flat spectrum in $]-\infty, \infty[$. As the flexural wave speed of the Kirchhoff model leads to infinite when the frequency leads to infinite, the flexural wave may appear anywhere on the plate at the same time of the impact. This phenomenon cannot be obtained physically since impact forces have a significant spectrum in a limited frequency ranges. Moreover, accurate plate model in the high frequency as the Mindlin one does not indicate infinite flexural wave speed for an infinite frequency. As in our numerical process, the spectrum is truncated to $[-f_{max}, f_{max}]$; these phenomena cannot be reproduced for the first times after the impact. Figure 2 compares the time signal of the velocity obtained directly using equation (14) with the signal obtained with our numerical process with $f_{max} = 40\ kHz$ and $\delta f = 1 Hz$. One can observe that both signals have similar shape, except for low times since frequencies higher than 40 kHz (which are the fastest waves) appear only on the analytical result. The damping effect and the dispersion of the flexural waves are correctly described with the numerical process.
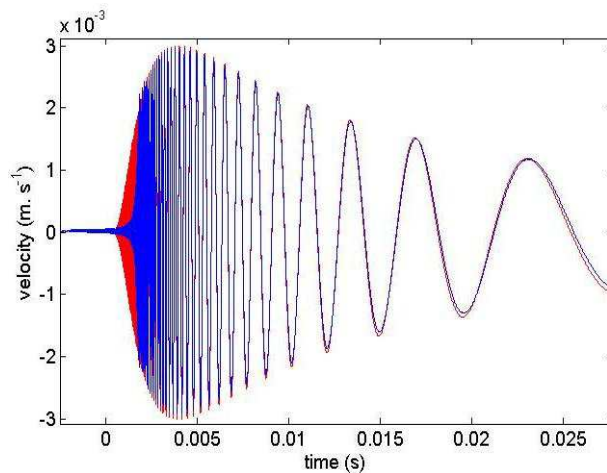

Figure 2 - Time signal of the velocity of the plate at r = 5 m; (——): analytical expression, (——): numerical process

4. ANALYSIS OF THE TIME RESPONSE OF THE FLUID LOADED PLATE

4.1 Vibratory response of the plate

4.1.1 Time signals of the displacement, of the velocity and of the acceleration

Usually, when we consider a stationary excitation, the spectra of the displacement and of the velocity can be easily deduced from the acceleration spectrum because these three quantities are related by a $-i\omega$ factor. In transient state, the time signal has different shape depending on the evaluated quantities as illustrated in Figure 3. The choice of the time scale (i.e. frequency resolution in our numerical process) and of the time resolution (i.e. sampling frequency in our numerical process) depend of the considered quantity. For instance, the observation of the displacement needs a larger time scale than the velocity and the acceleration. The acceleration will be considered in the following because it is the quantity generally measured by standard sensors (i.e. accelerometers) and it is directly related to the radiated pressure by the Euler equation (i.e. gradient of the pressure proportional to the acceleration).
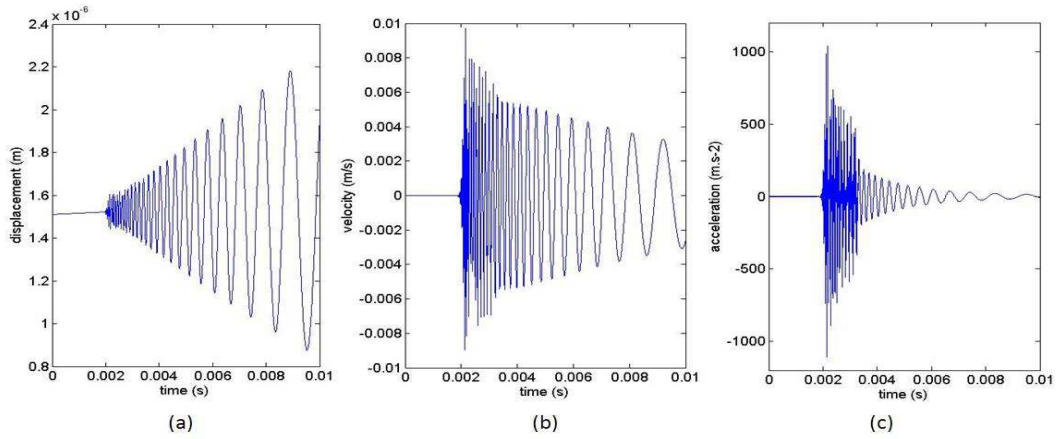

Figure 3 - Time signals obtained for: (a), displacement; (b), velocity; (c), acceleration

4.1.2 Effect of the fluid loading

The effect of the fluid loading on the plate vibration can be observed by comparing the response of the fluid loaded plate with the one of the in-vacuo plate. It is well known that the critical frequency, f_c (i.e. frequency at which the flexural wavelength is equal to the acoustic wavelength) plays an important role:

$$f_c = \frac{c_0{}^2}{2\pi}\sqrt{\frac{\rho_s h}{D}} \quad (14)$$

Below this frequency, the natural flexural waves radiate in the near field and are evanescent, the vibratory energy remains in the plate whereas above it, these waves radiate progressive waves which can be observed in the far field and the vibratory energy is strongly transmitted to the fluid. Figure 4 compares the acceleration of in-vacuo and fluid loaded plates in the wavenumber space at frequencies below and above f_c. The main peak is reached for the wavenumber γ equal to the natural flexural wavenumber of the plate, k_f. The added mass effect of the fluid is well observed below the critical frequency (i.e black curves) .

Below the critical frequency (i.e. green curve), we observe a valley at $\gamma = k_0$ and above f_c a peak appears at the same value of γ.
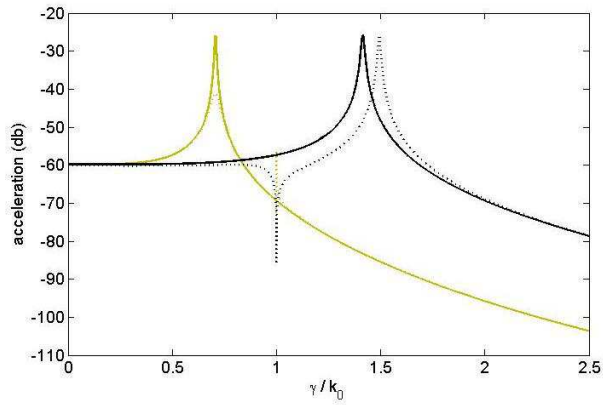
Figure 4 - Displacement of the fluid loaded (…) and in-vaccuo (—) plate in the wavenumber space at (—): f = 2f$_c$, (—): f = 0.5fc

The spectra of the accelerations of the in-vacuo plate and the loaded plate are compared in **Figure 5**. The effect of the critical frequency is observed as the amplitude falls in the case of the loaded plate. The phases of the velocities are also compared and it appears that both are similar below f$_c$, showing the dispersive nature of the flexural waves. However, above f_c the phase of the loaded plate velocity becomes linear. As the energy is mostly transferred to the fluid, the vibrations are induced more by the motions of the fluid than by the elastic behavior of the plate. The associated time signals obtained by inverse Time-Fourier transform are shown in Figure 6. The highest frequencies appear only for the in-vacuo plate since they are radiated into the fluid for the loaded plate. After the time t_a corresponding to the arrival time of the acoustic wave ($t_a = \frac{r}{c_0}$), both signals are similar since the vibratory energy remains in the loaded plate for the frequencies below f_c.
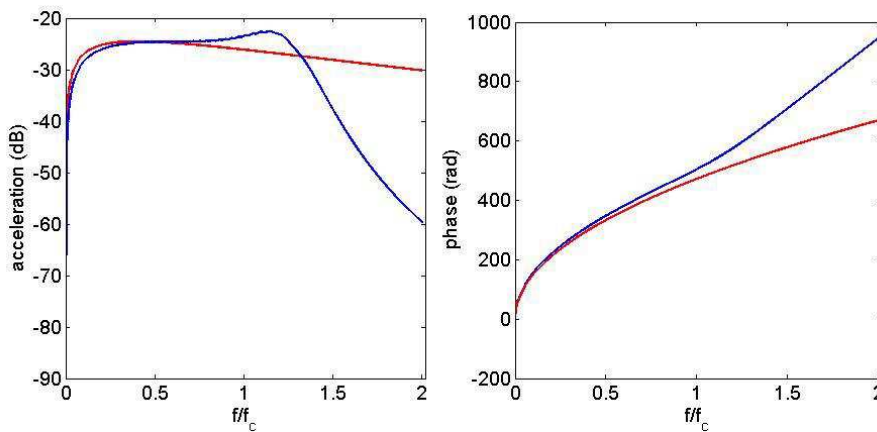

Figure 5 - Amplitude and phase of the plate acceleration spectra at r = 5 m; (—): in-vacuo plate, (—): fluid loaded plate
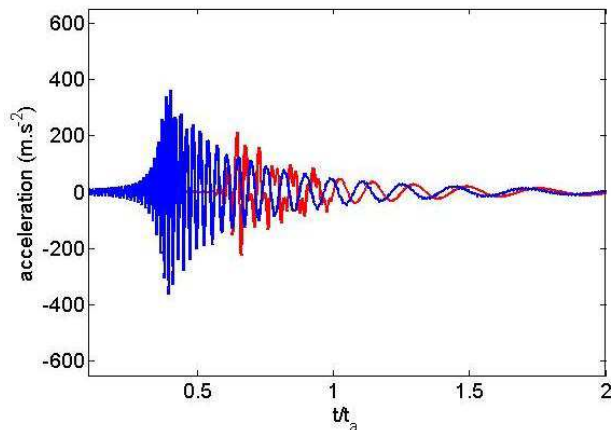

Figure 6 - Time signals of the plate acceleration at r = 5 m; (—): in-vacuo plate, (—): fluid loaded plate

4.2 Radiated pressure

In the far field of the plate, the radiated pressure can be obtained for a frequency in physical coordinates using the theorem of the stationary phase [11].

Analyzing the obtained expression in function of the angle ϕ shows that for a frequency $f_0 > f_c$ the radiated pressure is maximum for ϕ_0 :

$$\phi_0 = \sin^{-1}\sqrt{\frac{f_c}{f_0}} \qquad (15)$$

As shown in Figure 7, if we study the pressure spectra at different angles ϕ of observation, we can observe that the spectra reach a maximum peak at different frequencies. These frequencies can be estimated by calculating the frequency such that $\phi = \phi_0$.

Time responses are shown in Figure 8. The signal appears impulsively and decreases with an oscillation that contains one main frequency, since the others are filtered by the fluid. This frequency corresponds to the peak of the spectrum observed in Figure 7. It differs with the angle of observation as the maximum amplitude.
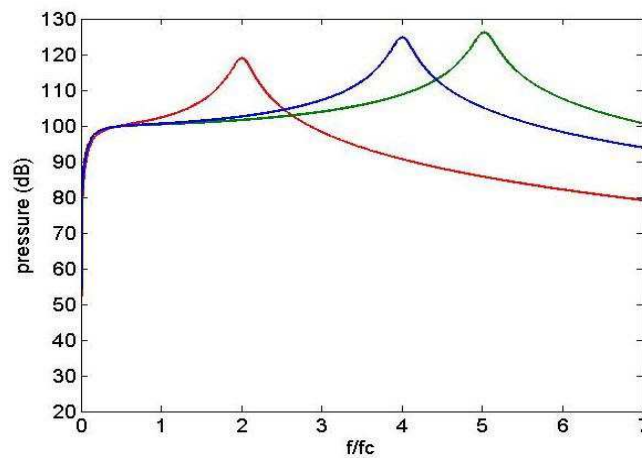

Figure 7 - Far field pressure spectra at R=10 m ; (—): $\varphi = 45°$, (—): $\varphi = 30°$, (—): $\varphi = 26,5°$
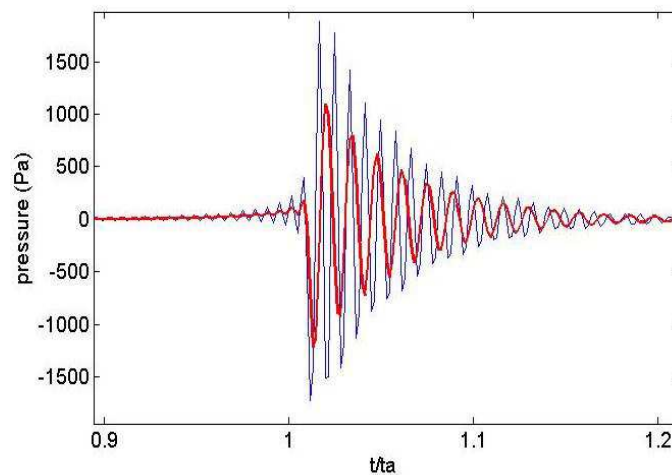

Figure 8 - Time signals of far field radiated pressure at R = 10 m, (—): $\varphi = 45°$, (—): $\varphi = 30°$

4.4 Influence of the plate model

We study in this section the influence of the rotational inertia and the shear stress. To do that, we compare the results of the Mindlin model with the ones of the Love-Kirchhoff model. The latter neglects the rotation inertia and the shear stress. Figure 9 shows the spectra and time signals of the accelerations evaluated with both plate models. The spectra are similar below the critical frequency, but above it the shear stress effect is more and more influent since the Mindlin plate spectra has the highest amplitude. The time signal of the Kirchhoff-Love plate arrives sooner than the Mindlin plate's. The shear stress affects then the wavespeed

on the plate especially at high frequency. The low frequencies are less affected since both signals are similar for larger times. The far field radiated pressure is evaluated and presented on Figure 10. It is compared with the pressure obtained with the Kirchhoff-Love plate. Under the critical frequency, the effect of the models does not appear, as both pressures are similar. However above the critical frequency the pressure peak appears at a higher frequency for the Mindlin plate and the level of the peak is lower for this same plate.
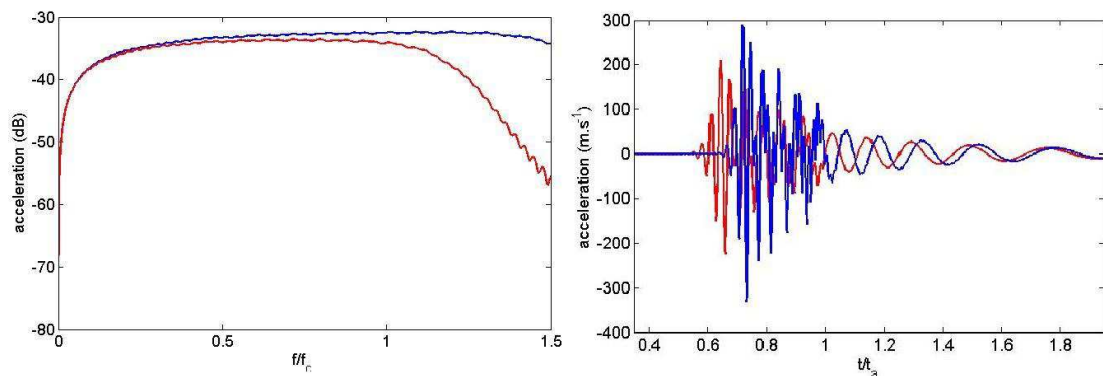

Figure 9 - Amplitude of the spectra (left) and time signals (right) of the plate flexural acceleration, (—): Kirchhoff- Love plate, (—): Mindlin plate
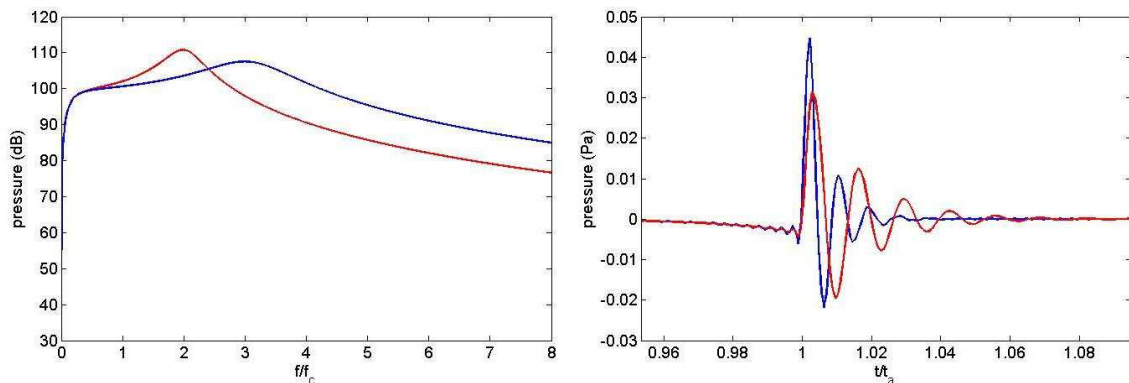

Figure 10 - Amplitude of the spectra (left) and time signals (right) of the far field radiated pressure; (—): Kirchhoff- Love plate, (—): Mindlin plate

5. CONCLUSIONS

An infinite plate excited by an impulse point force has been studied. After having validated the numerical process, we have analyzed the time response in term of plate acceleration and in term of radiated pressure in the far field. The influence on the time response of different phenomena/parameters such as the effect of the heavy fluid, the dispersion of the flexural waves, and the plate model has been highlighted. These results are going to be validated experimentally in a water tank. In the future, the numerical process considered in this paper could be applied to structures that are more similar to the concrete case of a submarine shell: a fluid loaded periodically stiffened panel [6-8] or an immersed shell coupled with its internal frames [9] could be considered.

REFERENCES

[1] Urick R J, *Principles of underwater sound 3rd ed.*, McGraw-Hill Inc., 423 p. (1983)
[2] Wang F, Mechefske C K, *Adaptive modeling of transient vibration signals* Mechanical Systems and Signal Processing, 20 p. 825-842 (2006)
[3] Mackertich S, Hayek S., *Acoustic radiation from an impulsively excited plate*, J. Acoust. Soc. Am, 69(4), p. 1021-1028 (1981)
[4] Choi S-H, Igusa T, Achenbach J D *Acoustic radiation from a finite-length shell with substructures subjected to an impulsive load*, Wave Motion, 22, p. 259-277 (1995)
[5] Leblond C, Iakovlev S, Sigrist J-F *A fully elastic model for studying submerged circular cylindrical shells subjected to a weak shock wave*, Mécanique & Industries, 10, p. 275-284, (2009)

[6] Rumerman M L, *Vibration and wave propagation in ribbed plates*. J. Acoust. Soc. Am., 57(2), 370–3, (1975)

[7] Maxit L, *Wavenumber space and physical space responses of a periodically ribbed plate to a point drive: A discrete approach,* Applied Acoustics, Vol 4, p 563-578, (2009)

[8] Mace B R, *Periodically stiffened fluid-loaded plates, I: response to convected harmonic pressure and free wave propagation*. Journal of Sound Vibration, 73(4), 473–86, (1980)

[9] Maxit L, Ginoux J-M, *Sound radiated by a submerged irregularly ribbed shell: the circumferential admittance approach,* Journal of the Acoustical Society of America, 128 (1), 137-151, (2010)

[10] Feit D, *Pressure Radiated by a point-Excited Elastic Plate*, J. Acoust. Soc. Am., 40(6), 1489-1494, (1951)

[11] Moler C B, *Numerical computing with MATLAB*, Society for Industrial Mathematics, (2004)

[12] Junger MC, Fiet D, *Sound, structures and their interaction, 2nd ed.*, Cambridge: The MIT Press, 448p. (1986)

[13] Guyomar D, Wang X J, Petit L, Lallart M, Monnier T, Yuse K, Audigier D, *Modeling of transient bending wave in an infinite plate and its coupling to arbitrary shaped piezoelements*, Sensors and Actuators A 171, p. 93-101 (2011)